

Supplementary information

Nickel Sulfide Cocatalyst-Modified Silicon Nanowire Arrays for Efficient Seawater-based Hydrogen Generation

Junjie Wang^{1,#}, Bo Wang^{1,2,#}, Xinmeng He^{1,#}, Jun Lv^{1,3,*}, Zhiyong Bao^{1,3}, Jiewu Cui^{1,3},
Guangqing Xu^{1,3,*} and Wangqiang Shen^{1,3,4,*}

¹*School of Materials Science and Engineering, Hefei University of Technology, Hefei 230009, China*

²*School of Physics, Nanjing University, Nanjing 210093, China*

³*Key Laboratory of Advanced Functional Materials and Devices of Anhui Province, Hefei University of Technology, Hefei 230009, China*

⁴*Engineering Research Center of High-Performance Copper Alloy Materials and Processing, Ministry of Education, Hefei University of Technology, Hefei, 230009, China*

[#]*These authors contributed equally to this work.*

^{*}Corresponding author.

E-mail addresses: lvjun@hfut.edu.cn (J. L.), gqxu1979@hfut.edu.cn (G. X.) and shenwq@hfut.edu.cn (W. S.)

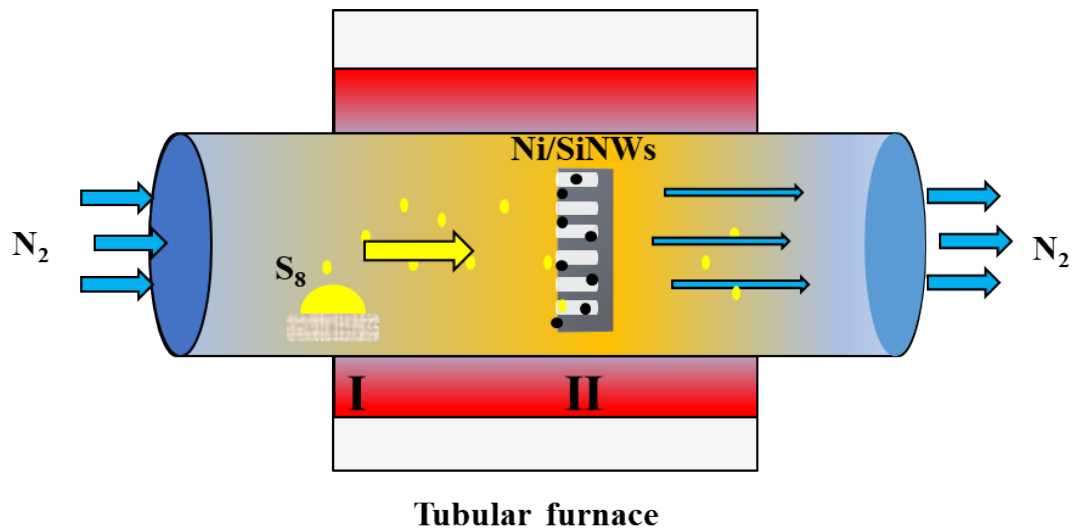


Figure S1. Schematic diagram of the preparation process for NiSi_x/SiNWs.

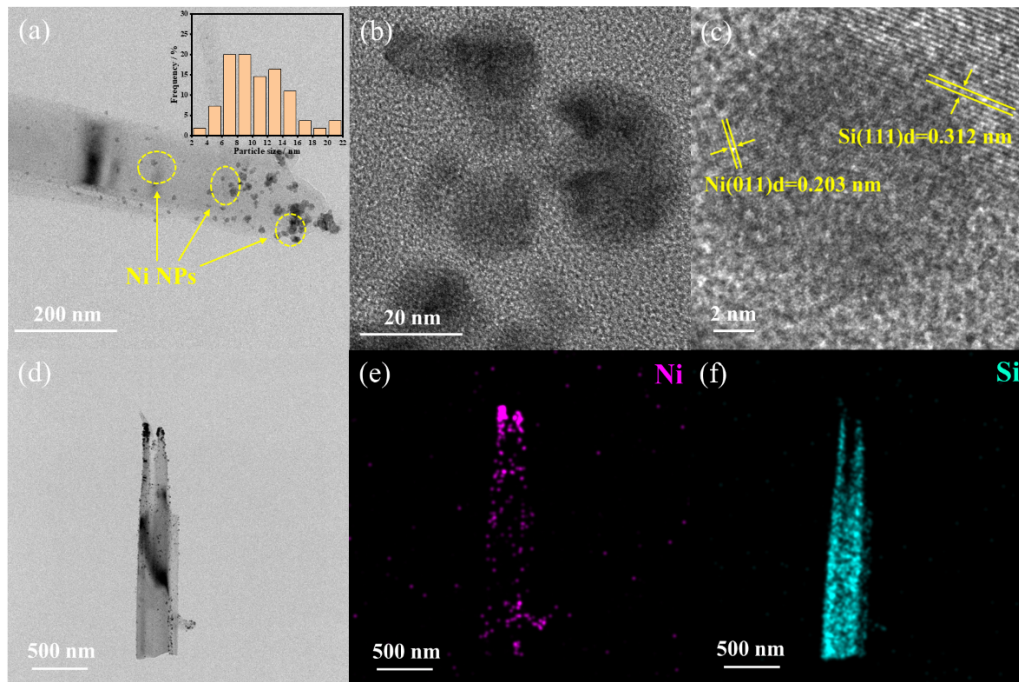


Figure S2. TEM image of Ni/SiNWs (a, b and d), HRTEM image (c), the corresponding elemental maps: (e) Ni and (f) Si.

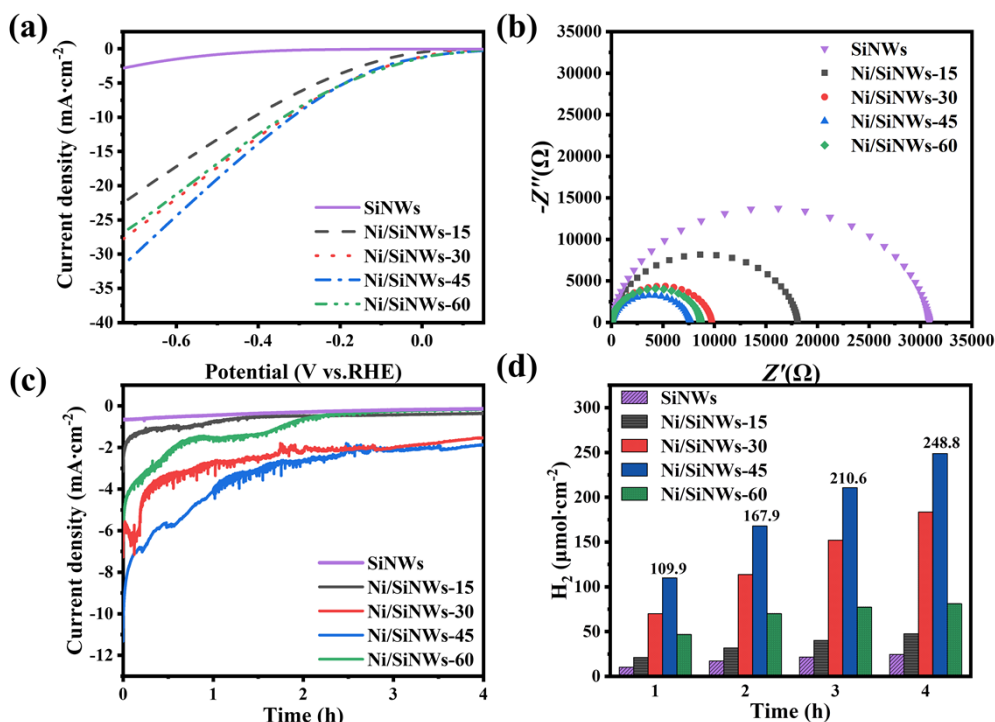


Figure S3. Photoelectrochemical hydrogen evolution performances of Ni/SiNWs: (a) Linear scanning voltammogram, (b) Nyquist impedance spectrogram, (c) PEC stability tests of SiNWs and Ni/SiNWs photocathodes in simulated seawater measured at -0.33 V vs. RHE under 100 mW·cm⁻² illumination and (d) the corresponding H₂ evolution performance of SiNWs and Ni/SiNWs photocathodes in simulated seawater.

The as-fabricated SiNWs and Ni/SiNWs photocathodes were performed under photoelectrochemical test. As Figure S3a shows, the current density of Ni/SiNWs are significantly higher than SiNWs photocathode under the same potential, which illustrates the superior electrocatalytic activity of Ni nanoparticles. The Ni/SiNWs-45 exhibits the optimum performance, while further increasing the deposition time of Ni, the performance of Ni/SiNWs declines, which may be ascribed to the agglomeration of Ni nanoparticles. Figure S3b is the Nyquist spectra of Ni/SiNWs with different deposition times, the decreased radius of Ni/SiNWs compared to SiNWs also indicates the faster carriers transfer property at the solid/electrolyte interface. The long-time photoelectrochemical performance is illustrated in Figure S3c, all Ni/SiNWs photocathodes exhibits higher current density than SiNWs illustrating the electrocatalytic activity of Ni NPs. However, the performance of Ni/SiNWs photocathode gradually decrease, which could be ascribed to the oxidation of Ni NPs during the PEC process. The Ni 2p XPS result of Ni/SiNWs photocathode after PEC process for 4h also convinced that the Ni²⁺ peak increases and the Ni⁰ peak disappears (Figure S4). The corresponding H₂ evolution amount was obtained in Figure S3d, the optimized Ni/SiNWs-45 photocathode exhibits H₂ yield rate of 62.2 μmol·h⁻¹·cm⁻², while the unloaded SiNWs photocathode is only 6.13 μmol·h⁻¹·cm⁻². Thus, the instability of Ni nanoparticles hampers its application on PEC HER process, although it's excellent catalytic activity.

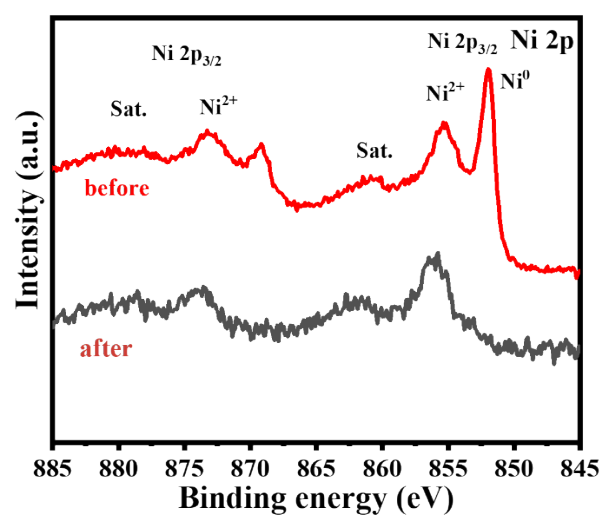


Figure S4. XPS spectrum of Ni 2p in Ni/SiNWs after photoelectrochemical hydrogen evolution process.

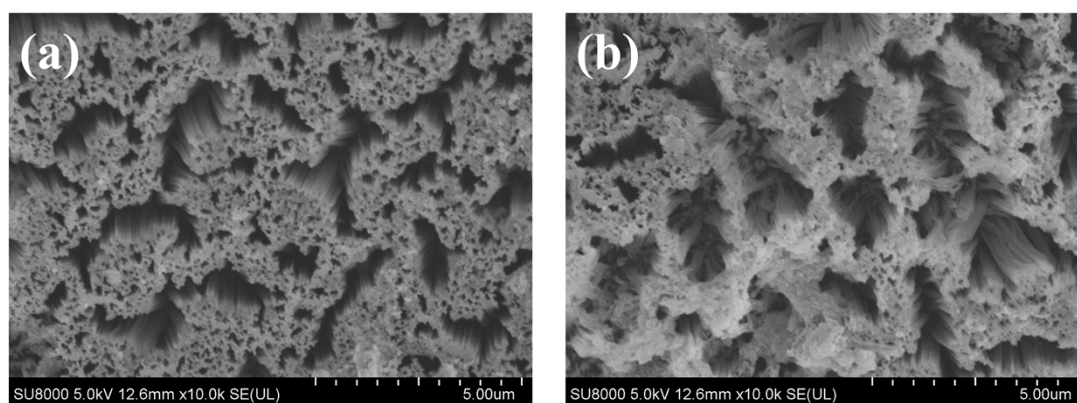


Figure S5. SEM images of NiS_x/SiNWs: (a) before photoelectrochemical hydrogen evolution process, (b) after photoelectrochemical hydrogen evolution process.

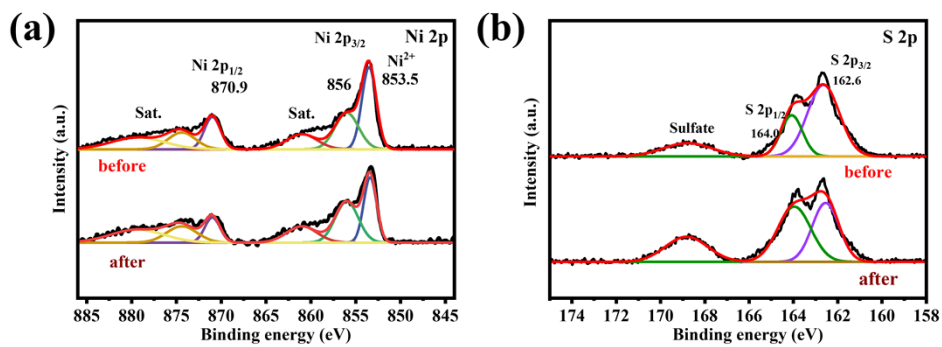


Figure S6. High resolution XPS spectra of (a) Ni 2p and (b) S 2p in NiS_x/SiNWs after photoelectrochemical hydrogen evolution process.

Table S1. Fitting results of EIS curves for SiNWs and NiS_x/SiNWs samples

Samples	R _s	R _{ct}	CPE-T	CPE-P
SiNWs	45.22	21072	1.407×10 ⁻⁵	0.995
NiS _x /SiNWs	22.58	4994	6.607×10 ⁻⁵	0.802

Table S2. Comparison with the similar reported works in literature

Photocathode	Electrolyte	Hydrogen evolution potential at $-10 \text{ mA}\cdot\text{cm}^{-2}$ (V vs. RHE)	V vs. RHE/ H_2 evolution rate($\mu\text{mol}\cdot\text{h}^{-1}\cdot\text{cm}^{-2}$)	Refs
NiS_x/SiNWs	simulated seawater	-0.316	-0.33/189.15	This work
RuCo@Ti	simulated seawater	-0.387	~	1
PtNi _x	natural seawater	-0.38	~	2
Co ₃ O ₄	natural seawater	-0.950	~	3
SiNWs@MoS ₂ /NiS ₂	0.5 mol·L ⁻¹ Na ₂ SO ₄	-0.560	-0.50/183	4
MoS ₂ /SiNWs	0.5 mol·L ⁻¹ H ₂ SO ₄	-0.300	0/226.5	5
PANI/GO/TiO ₂	simulated seawater	~	0.07/72.5	6
AlGaN/ GaN heteroepitaxial films	natural seawater	~	-0. 4/95	7

References

1. X. M. Niu, Q. W. Tang, B. L. He and P. Z. Yang, Robust and stable ruthenium alloy electrocatalysts for hydrogen evolution by seawater splitting, *Electrochimica Acta*, 2016, **208**, 180-187.
2. J. J. Zheng, Seawater splitting for high-efficiency hydrogen evolution by alloyed PtNi_x electrocatalysts, *Applied Surface Science*, 2017, **413**, 360-365.
3. M. Patel, W. H. Park, A. Ray, J. Kim and J. H. Lee, Photoelectrocatalytic sea water splitting using Kirkendall diffusion grown functional Co₃O₄ film, *Solar Energy Materials and Solar Cells*, 2017, **171**, 267-274.
4. F. F. Lin, R. R. Tian, P. Dong, G. F. Jiang, F. T. He, S. J. Wang, R. B. Fu, C. C. Zhao, Y. Y. Gu and S. B. Wang, Defect-rich MoS₂/NiS₂ nanosheets loaded on SiNWs for efficient and stable photoelectrochemical hydrogen production, *Journal of Colloid and Interface Science*, 2023, **631**, 133-142.
5. B. Wang, H. N. Wu, G. Q. Xu, X. Y. Zhang, X. Shu, J. Lv and Y. C. Wu, MoS_x quantum dot-modified black silicon for highly efficient photoelectrochemical hydrogen evolution, *ACS Sustainable Chemistry & Engineering*, 2019, **7**, 17598-17605.
6. X. Y. Yuan, Y. Xu, H. Meng, Y. D. Han, J. B. Wu, J. L. Xu and X. Zhang, Fabrication of ternary polyaniline-graphene oxide-TiO₂ hybrid films with enhanced activity for photoelectrocatalytic hydrogen production, *Separation and Purification Technology*, 2018, **193**, 358-367.
7. M. L. Lee, P. H. Liao, G. L. Li, H. W. Chang, C. W. Lee and J. K. Sheu, Enhanced production rates of hydrogen generation and carbon dioxide reduction using aluminum gallium nitride/gallium nitride heteroepitaxial films as photoelectrodes in seawater, *Solar Energy Materials and Solar Cells*, 2019, **202**, 110153.